Hindawi
Shock and Vibration
Volume 2023, Article ID 4140583, 17 pages
https://doi.org/10.1155/2023/4140583

Research Article

Analytical Model of Structural Damping in Friction Module of Shell Shock Absorber Connected to Spring

Ivan Shatskyi[1] **and Andrii Velychkovych**[2]

[1]*Laboratory of Modeling of Damping Systems, Pidstryhach-Institute for Applied Problems in Mechanics and Mathematics of the National Academy of Sciences of Ukraine, Mykytynetska Street 3, Ivano-Frankivsk 76002, Ukraine*
[2]*Ivano-Frankivsk National Technical University of Oil and Gas, Karpatska Street 15, Ivano-Frankivsk 76019, Ukraine*

Correspondence should be addressed to Andrii Velychkovych; a_velychkovych@ukr.net

Received 8 July 2022; Revised 20 January 2023; Accepted 24 February 2023; Published 4 March 2023

Academic Editor: Wai-on Wong

Vibration processes play a significant role in the modern industry. In most cases, vibration reduces strength, reliability, and durability of industrial machines, mechanisms, and structures, as well as adversely affects the health of support staff. This study presents a new dry friction shell shock absorber design. The shock absorber contains two spring sections and a friction module with an open shell and an elastic filler; at the same time, the spring sections and the friction module work in parallel. The proposed device demonstrates good damping characteristics, capable of operating under high operating loads, and at the same time has compact transverse dimensions. With a nonmonotonic loading of such a shock absorber, due to the contact interaction of the filler with an open shell, part of the energy that is supplied to the system will be dissipated. In other words, in response to the action of an external nonmonotonic loading, the phenomenon of structural hysteresis occurs in the friction module of the shock absorber. To describe the deformation of the shock absorber, a mechanical and mathematical model of a shell with a cut along the generatrix, which is the main bearing link, has been developed. By means of the technique of quasistatic analysis of structural damping in nonmobile nonconservative shell systems with a deformable filler, the hysteresis loops of the presented shock absorber are analytically described. Using them, according to the known loading history, it is possible to predict the behavior of the considered nonconservative system at any time after the start of the loading process. At each stage of the cyclic loading, the distribution of stresses and relationships between the external loading and the piston displacement was studied. Inequalities are obtained for permissible loads under which the operation of the shock absorber is safe. Such shell shock absorbers are projected to be used in the mining, oil and gas, and construction industries.

1. Introduction

Vibration processes that occur in the operation of almost all, without exception, modern machines, and mechanisms, typically lead to undesirable consequences. In the vast majority of cases, vibration decreases the strength, reliability, and durability of industrial machines, mechanisms, and structures, as well as affects the health of personnel. This is why the research and design works and theoretical investigations in the field of development of new means of vibration protection and methods for their numerical analyses are of crucial importance [1].

Today, the problems of vibration isolation of objects and vibration damping remain relevant for a number of branches of mechanical engineering, instrumentation, and construction [2, 3]. In particular, in oil and gas drilling techniques, a drill string is a long structure connecting downhole tools and a drilling rig. Its dynamic characteristics are one of the key factors affecting the efficiency and cost of drilling [4]. Innovative mining technologies involve the use of a standard tool for complex operations, often associated with abnormal dynamic loadings [5, 6]. The specifics of the operation of drill strings [7] and sucker rod strings [8] lead to vibration loadings of downhole equipment, which can lead to

emergency situations [9]. Particular attention should be paid to the problems associated with premature failure, loss of tightness, and unintentional self-loosening of threaded connections due to exposure to intense vibrations [10]. This phenomenon can lead to significant financial losses due to the need for regular maintenance of threads and cause emergency situations [11, 12]. In this regard, the task of ensuring effective vibration protection of objects, as well as ensuring their isolation from shock impact, has always been and remains extremely relevant.

The global direction of solving the formulated problem is the use of highly specialized vibration protection devices–shock absorbers [13], dampers [14], elastic couplings, and dynamic absorbers [15]. As for traditional vibration dampers (hydraulic, metal, rubber), the market offers a wide variety of technical solutions, and their properties have been studied at a level sufficient for engineering practice. Due to the development of new technologies, attempts to introduce magnetorheological fluid dampers [16], regenerative shock absorbers [17], and vibration dampers with electromagnetic damping [18] are becoming more frequent. The energy-harvesting technology using the vibration energy can be divided into piezoelectric, electrostatic, and electromagnetic methods [19]. In paper [20], a mechatronic shock absorber based on ball screw pair is designed, which can produce a large damping force. The study [21] proposes a novel design of a regenerative shock absorber for the in-wheel motor to capture the vibration energy from the rough road surface while driving an electric vehicle. A novel hydraulic energy harvesting interconnected shock absorber is proposed in paper [22] to improve the efficiency of energy harvesting, ride comfort, and road handling performance. New methods as use of the magnetorheological elastomer (a smart material with elastic property variable in the external magnetic field) were developed in the last period to absorb the vibration energy [23].

Separately, it is necessary to pay attention to vibration-dampening systems in the construction industry. High-rise structures are vulnerable to structural vibrations induced by wind and earthquake loadings [24]. Passive-tuned mass and liquid dampers are a popular choice among structural vibration control systems for being reliable, economical, and easy to implement [25]. Passive vibration control devices like tuned liquid column dampers not only significantly reduce buildings' vibrations but also can serve as a water storage facility [26]. Particular interest is aroused by the dynamic damper designs based on the effect of collisions [27, 28]. The dynamic conditions of the object connected with a vibration-impact damper are changed both by a redistribution of vibration energy from the object to the damper and by an increase in the vibration energy dissipation [29]. There exists an optimum filling ratio and mass ratio in which the damper can reach the best damping state [27, 30].

Due to the simplicity of designs and inexpensive maintenance, engineers often prefer shock absorbers and dampers with dry friction when designing modern vibration protection systems [31, 32]. Friction dampers are devices that use dry friction to dissipate the energy of a system in order to limit its vibratory response. They work by keeping in contact wih two surfaces that move relative to each other in order to generate friction [33]. The use of friction dampers has been widely proposed for a variety of mechanical systems for which applying viscoelastic materials, fluid-based dampers, or other viscous dampers is impossible. An important example is the application of friction dampers in aircraft engines to reduce the blades' vibration amplitudes [34]. Recurrent impact protection devices usually need to dissipate large amounts of energy to prevent damage to the infrastructure they protect. The device proposed in article [35] is composed of rigid parts with articulated joints, an elastic element that allows the recovery of its shape, and an element that dissipates energy by friction. Dry friction damping technology is an effective means of cardan drives of helicopter tail rotors [36]. Friction effects in the so-called Coulomb damper are widely used in material mixing equipment and automatic washing machines [37]. A number of designs of friction dampers have been developed to improve the seismic characteristics of industrial and civil structures [38]. When compared to other means to attenuate vibration, friction dampers stand out by their advantages. To name a few, they work in harsh environments and in the absence of electric or hydraulic power, and they adapt to a wide excitation bandwidth without tuning [33].

Minimum overall dimensions and weight, stability of vibration protection properties, manufacturability, operational reliability, and low cost are well-known requirements for a modern vibration protection system. In addition, when designing vibration protection devices for systems experiencing extreme loadings, it is necessary to strive for a combination of the high bearing capacity of the structure with relatively low rigidity and the required level of damping. In the case of a strict limitation imposed on the transverse dimension of the vibration isolator, for vibration protection of heavily loaded objects in the mining, metallurgical, construction, and oil and gas industries, we propose to use the original design of the shell shock absorber (Figure 1(a)). The main feature of the proposed design is the use of an open cylindrical shell as the main working link, which provides excellent damping characteristics for the device. In the shock absorber, together with the shell module, two additional spring sections operate in parallel, which makes it possible to provide the required load-bearing capacity of the shock absorber.

In Figure 1(b), the shock absorber works as follows. External axial loading is perceived by pistons 2, which compress filler 3 and compression springs 4. Filler transforms longitudinal displacements of pistons 2 into radial deformations of shell 1. The open shell 1 and the compression springs 4, deforming within the limits of elasticity, accumulate energy and, when the external loading disappears (or decreases), return pistons 2 to their original (or intermediate) position. In this case, part of the energy supplied to the shock absorber is dissipated mainly due to mutual slippage with the friction of the filler and the shell. It is important that all three bearing links of the elastic element (shell with a cut 1 and two compression springs 4) will work in parallel; that is, in general, their holding capacity is summed up, and each of these links will carry a share of the

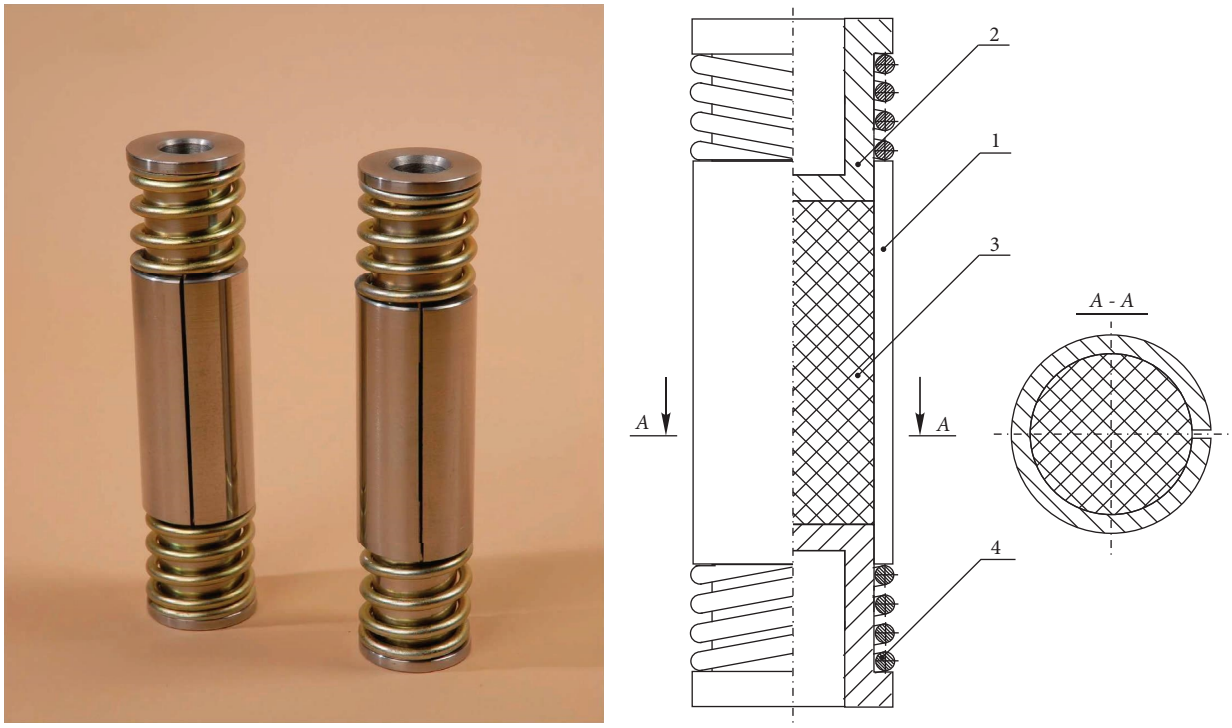

Figure 1: Friction shock absorber with open shell: (a) full-scale shock absorber samples; (b) a circuit diagram of the shock absorber; 1: shell with a cut along the generatrix; 2: piston; 3: elastic filler; 4: helical compression spring.

external loading proportional to its own rigidity. The tribological properties of the filler-shell pair are selected for reasons of providing the level of structural damping required in a particular operational situation.

From the point of view of mechanics, the proposed shock absorber is a nonconservative deformable system with dry friction [39, 40]. When performing mathematical modeling of the behavior of such systems under the influence of a nonmonotonic loading, nonlinear contact problems arise on the frictional interaction of shells with elastic bodies [41, 42].

The contact interaction of real bodies is one of the most common and complex natural phenomena. The problems of contact mechanics are of great interest to researchers as a result of their practical application in the field of mechanical engineering [43, 44], the construction industry [45, 46], biomechanics, etc. [47, 48]. In general, when solving contact problems, researchers pay considerable attention to the analysis of the strength, rigidity, and stability of the contacting elements [49, 50]. Numerical-analytical models of the contact interaction of deformable systems with the environment are considered in studies [51–53]. A class of problems related to the effect of contact interaction of cut faces during the bending of thin shells is topical [54–58]. Similar problems, in which simultaneous loadings of plates and shells by tension (compression) and bending are considered, were solved in [59–61]. The elastic and boundary equilibrium of thin-walled structures on an elastic basis, in which cuts are present, was studied in publications [62, 63]. The works [64–67] are devoted to the study of dynamical systems with different laws of friction.

With a nonmonotonic loading of the friction shock absorber (Figure 1), as a result of the contact interaction of the filler with an open shell, the part of the energy supplied to the system will be dissipated. In other words, in response to the action of an external nonmonotonic loading, the phenomenon of structural hysteresis occurs in the friction shock absorber. Systems of passive and active damping of vibrations in mechanical engineering and construction were considered in the works [68–70]. The studies [71, 72] considered the phenomena of magnetostriction and internal damping in metals and alloys. A detailed review of the hysteresis properties of composites with a polymer matrix was carried out in [73], and an analysis of damping structures fabricated using modern additive technologies was carried out in [74]. Various models of structural damping and practical approaches to quantifying the energy dissipation of vibrations of structures equipped with dampers are presented in articles [75–77].

Practical experience and experimental studies [78–80] have shown that the use of open shells in shock absorbers can significantly reduce their rigidity compared to continuous shells [81, 82] and, as a result, reduce the resonant frequencies of a dynamic system. It is predicted that such shock absorbers will be especially useful when used in vibration machines of superresonance action in the foundry for vibration protection of drill strings and sucker rod strings. Such a conducive forecast for a wide range of

applications of the developed shock absorber became the main motivator of our research.

The aim of our study is to obtain an analytical description of the deformation diagram "external loading-draft" for the presented friction shock absorber. With the help of such a diagram, according to the known history of the loading, it is possible to predict the behavior of the considered nonconservative system at any time after the start of the loading process, as well as calculate the amount of energy dissipated in this case. At the same time, it is planned to investigate the distribution of stresses in the friction module of the shock absorber at each stage of the cyclic loading. To achieve the aim, the following tasks must be solved: to develop a mechanical-mathematical model of an open cylindrical shell, to perform the formulation, to obtain a solution to the problem of structural damping during the contact interaction of the deformable filler and the open shell, taking into account the presence of friction between them, and analytically to describe the process of drawing a deformation diagram of the shell shock absorber taking into account the parallel connection of the friction module and springs.

2. Materials and Methods

2.1. Mechanical and Mathematical Model of an Open Shell. To describe the deformation of a friction shock absorber, we first construct a mechanical-mathematical model of a shell with a cut along the generatrix, which is the main bearing link of the shock absorber (Figure 1(b)). Let us take into account the main feature of the design, the rigidity of the cut shell in the tangential direction is significantly less than along the generatrix. The main contribution to the compliance of the system will be made by changing the shape of the filler due to the bending deformation of the cut shell (reducing the curvature of the open ring in the cross section). Therefore, the following assumptions are logical. The filler material is assumed to be incompressible. To a cut isotropic shell that bends under conditions of a non-axisymmetric contact loading, we put in correspondence a strongly closed orthotropic cylindrical shell under the action of an axisymmetric contact loading (Figure 2). We keep the thicknesses and radii of the shells the same. We choose the elastic modulus for an equivalent orthotropic shell such that it identifies, on average, the properties of the cut shell and its continuous model.

To do this, we carry out a thought experiment. Let E_0 be Young's modulus for the material of the cut shell (Figure 2(a)). Let us denote by E_e the modulus of elasticity of the equivalent model to be determined (Figure 2(b)). Let us subject both shells to the action of internal pressure q and find deformations and displacements. We will use the cylindrical coordinate system r, ϑ, z (axis z in Figure 2 is not shown, and it is directed along the axis of the shell). As a result of the predominant effect of bending deformation, we will additionally assume that the middle surface of the cut shell is inextensible, and the middle surface of the orthotropic shell is stretched only in the tangential direction.

Taking into account the accepted assumptions, we will solve the plane problem of the loading of an open shell by internal pressure. The equilibrium equations have the following form:

$$\begin{aligned} \frac{dN_\vartheta}{d\vartheta} + Q_\vartheta &= 0, \\ \frac{dQ_\vartheta}{d\vartheta} - N_\vartheta &= -qR, \\ \frac{dM_\vartheta}{d\vartheta} - Q_\vartheta R &= 0, \\ \vartheta &\in (0, 2\pi), \end{aligned} \tag{1}$$

where N_ϑ is a tangential force, and M_ϑ and Q_ϑ denote bending moment and transverse force.

Having integrated the system of equation (1) under the boundary conditions:

$$N_\vartheta = 0, M_\vartheta = 0, Q_\vartheta = 0 \text{ when } \vartheta = 0, 2\pi. \tag{2}$$

We obtain expressions for forces and moments:

$$\begin{aligned} N_\vartheta &= 2qR \sin^2\left(\frac{\vartheta}{2}\right), \\ Q_\vartheta &= -qR \sin\vartheta, \\ M_\vartheta &= -2qR^2 \sin^2\left(\frac{\vartheta}{2}\right). \end{aligned} \tag{3}$$

We find the deflection function by the differential equation

$$\frac{d^2w}{d\vartheta^2} + w = -\frac{12R^2}{E_0h^3}M_\vartheta, \quad \vartheta \in (0, 2\pi). \tag{4}$$

Integrating expression (4), we have

$$w(\vartheta) = A\cos\vartheta + B\sin\vartheta + \frac{12qR^4}{E_0h^3}\left(1 - \frac{1}{2}\vartheta\sin\vartheta\right). \tag{5}$$

Here, the first two summands describe the movement of the section of an open shell as a rigid body. Now, we find the average value of the bending

$$\frac{w^{(1)}}{R} = \frac{1}{2\pi}\int_0^{2\pi}\frac{w(\vartheta)}{R}d\vartheta = \frac{18qR^3}{E_0h^3}. \tag{6}$$

In an orthotropic momentless shell, a tangential force arises under the action of internal pressure $N_\vartheta = qR$. For tangential deformation, we will have the following expression:

$$\frac{w^{(2)}}{R} = \frac{q}{E_e}\frac{R}{h}. \tag{7}$$

Requiring that the average deflections in the left parts of expressions (6) and (7) be the same, we find the equivalent elastic constant of the model continuous shell:

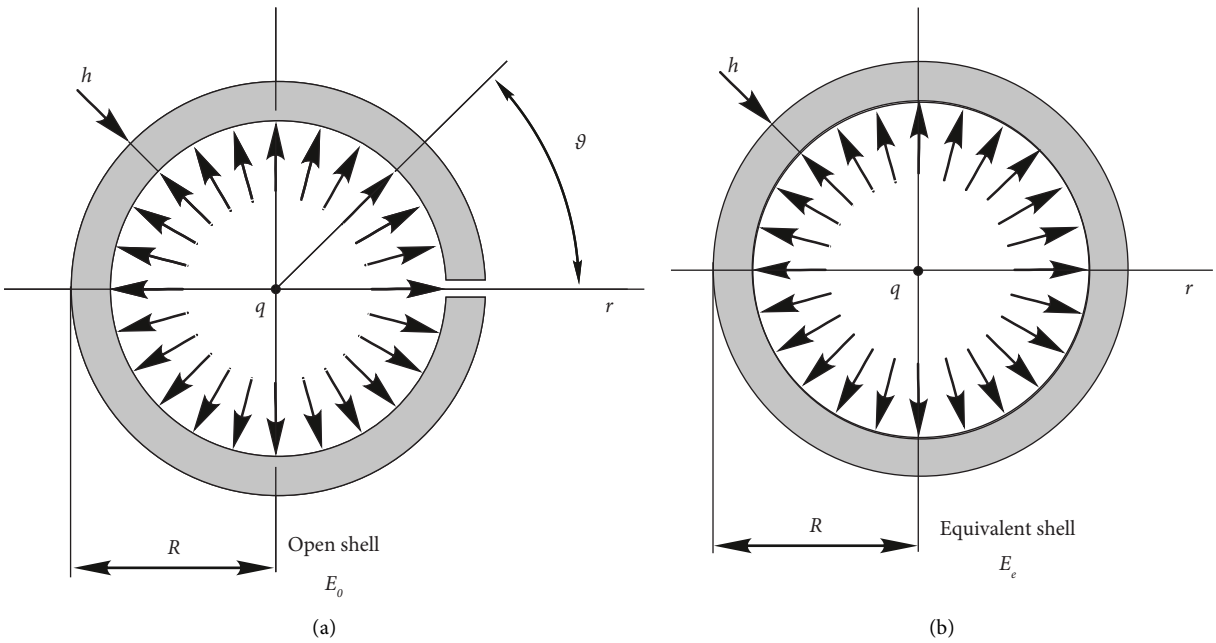

Figure 2: Scheme of a thought experiment for constructing an open shell model: (a) isotropic open shell; (b) equivalent orthotropic closed shell.

$$E_e = \frac{1}{18}\frac{h^2}{R^2}E_0. \tag{8}$$

2.2. Analytical Model of Structural Damping in a Friction Shock Absorber. Let us consider structural damping in a model strongly orthotropic shell with a deformable filler. In view of the symmetry of the structure with respect to a plane equidistant from the pistons, we will study half of the system (Figure 3), considering the section belonging to the plane of symmetry to be supported by a rigid barrier. Therefore, we have an elastic incompressible deformable cylinder (filler), with the radius R and length a, which fills a strongly orthotropic shell of thickness h. A linear compression spring is installed between the piston collar and the end face of the shell. An external cyclic loading Q is applied to an absolutely rigid smooth piston. The nature of the contact interaction of the shell and filler is determined by the law of dry friction. Let us study the energy dissipation in a frictional contact.

The frequency-dependent energy dissipation that occurs due to internal friction in the filler is negligible compared to amplitude-dependent structural damping during contact sliding. Therefore, the viscosity of the filler material is not taken into account.

The initial model relations for the filler will be the equation of equilibrium, equation of incompressibility, and Hooke's law for incompressible material averaged over the cross-sectional area

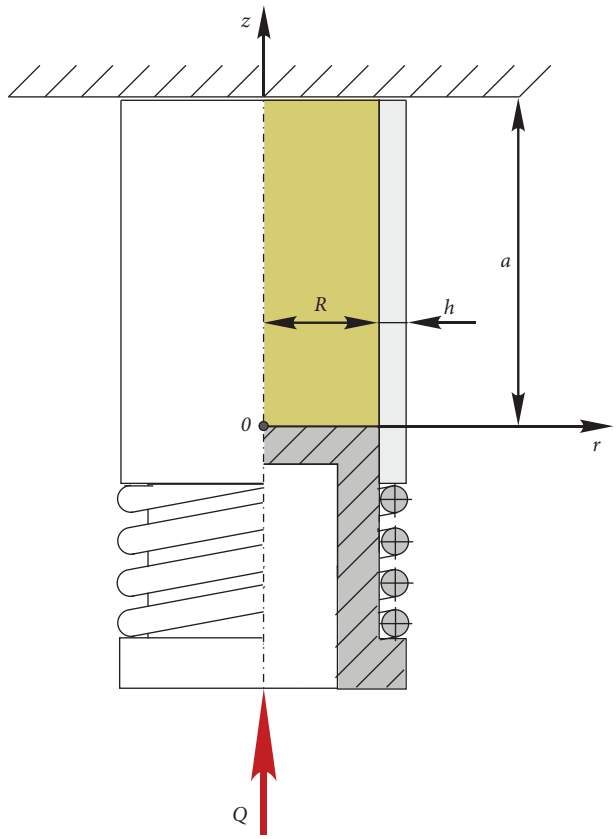

Figure 3: Calculation scheme of a friction shock absorber.

$$\frac{d\sigma_\zeta}{d\zeta} + 2\frac{a}{R}\tau = 0,$$

$$\frac{du}{d\zeta} + 2\frac{a}{R}w = 0, \tag{9}$$

$$\frac{du}{d\zeta} = \frac{a}{E}\left(\sigma_\zeta - \sigma\right), \quad \zeta \in (0,1),$$

where σ_ζ, u are axial stresses and filler displacement, σ and τ are normal and tangential contact stresses, w denotes radial displacement on the surface $r = R$, E denotes Young's modulus of the filler material, and $\zeta = (z/a)$ is a dimensionless coordinate.

For a model orthotropic shell, describing its elastic equilibrium by the relations of the momentless theory, and assuming that its middle surface is stretched only in the tangential direction, we have

$$w_0 = -\frac{\sigma R^2}{E_e h}, u_0 = 0, \quad \zeta \in (0,1), \tag{10}$$

where w_0, u_0 are radial and axial displacement of the shell; E_e is an equivalent elastic constant determined by the formula (8).

The frictional interaction of the shell and filler is described by the relations of one-sided contact and Coulomb's law of dry friction in a quasi-static interpretation:

$$w_0 = w, \sigma < 0,$$

$$\tau = f\sigma \operatorname{sgn}\frac{\partial u}{\partial Q}\dot{Q}, \frac{\partial u}{\partial Q} \neq 0, |\tau| \leq -f\sigma, \frac{\partial u}{\partial Q} = 0, \tag{11}$$

where f is a coefficient of friction of the shell-filler contact pair.

To find the coordinates of the point of delimitation of the areas of adhesion and sliding, α it is necessary to use the condition of continuity of axial stresses in the filler:

$$\sigma_\zeta(\alpha - 0) = \sigma_\zeta(\alpha + 0). \tag{12}$$

Let us now consider the situation at the end of the filler. With parallel connection, the external loading on the piston is divided into two parts

$$Q = Q_1 + Q_2, \tag{13}$$

where Q_1 is a filler loading, and Q_2 denotes a spring loading.

The first of them is proportional to the unknown pressure p under the piston, and the second is proportional to the displacement of the extreme coil of the spring $u_2(0)$:

$$Q_1 = p\pi R^2,$$
$$Q_2 = c_2 u_2(0). \tag{14}$$

Here, c_2 is a coefficient of linear rigidity of the spring. Given that under the piston

$$p = -\sigma_\zeta(0),$$
$$u_2(0) = u(0). \tag{15}$$

From formulas (13)–(15), we obtain the boundary condition at the lower end of the filler:

$$Q = -\sigma_\zeta(0)\pi R^2 + c_2 u(0). \tag{16}$$

The upper end of the cylinder is stationary:

$$u(1) = 0. \tag{17}$$

Therefore, the boundary value problem of the contact interaction of the shell and filler, taking into account the forces of dry friction, is formulated. We built its solution separately for each of the sections–sliding and ideal adhesion at each stage of the cyclic loading.

3. Results and Discussion

First, let us consider the cyclic deformation of the "filler-shell" subsystem under some loading Q_1 with cycle asymmetry coefficient $s = Q_{1\min}/Q_{1\max} \equiv p_{\min}/p_{\max} \in [0,1]$. The process of nonmonotonic loading was divided into stages where the loading is monotonic. As a result of solving problem (9)–(12), (16), and (17) according to the method started in [41, 70], we obtained expressions for contact σ, τ and axial σ_ζ stresses and piston displacements δ at all stages of loading. Let's present the solutions of the problem for each stage separately.

For clarity of notation, we introduce an additional superscript Roman index. The number I will indicate the stage of active (initial) loading, the number II will indicate the stage of unloading, and the number III will indicate the stage of repeated loading.

3.1. The Stage of the Initial (Active) Load of the Shock Absorber. Shock absorber load parameters are $0 \leq p \leq p_{\max}, \dot{p} > 0, \partial u/\partial p > 0$.

At the initial stage of loading, contact and axial stresses are described by the following formulas:

$$\sigma^I(\zeta) = -\frac{p}{1+2\varepsilon}e^{-\lambda\zeta},$$

$$\tau^I(\zeta) = -\frac{fp}{1+2\varepsilon}e^{-\lambda\zeta}, \tag{18}$$

$$\sigma_\zeta{}^I(\zeta) = -pe^{-\lambda\zeta},$$

$$\zeta \in [0,1],$$

where $\lambda = 2f(a/R)(1/(1+2\varepsilon))$ is parameter of exponential decay of axial and contact stresses; $\varepsilon = 18(E/E_0)(R^3/h^3)$ is auxiliary dimensionless rigidity parameter.

Graphically, these dependencies are shown in Figure 4. Here and below, to illustrate the results obtained, as an example, a system with parameters $f = 0.5$, $a/R = 3$, $h/R = 0.18$, $E/E_0 = 10^{-4}$. Then, $\varepsilon \approx 0.31$, $\lambda \approx 1.86$. The selected numerical parameters correspond to real samples of shock

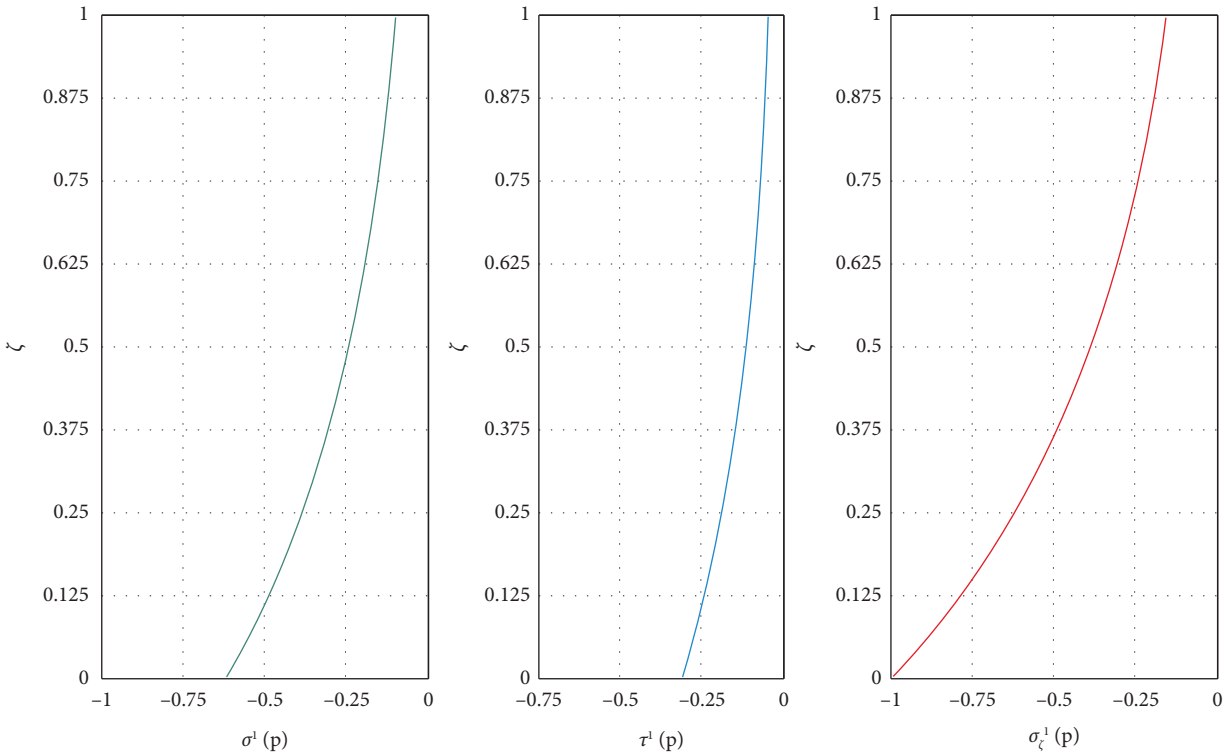

Figure 4: Stress distribution at the active loading stage.

absorbers for the elastic suspension of the sucker rod string [8].

If we trace the behavior of contact and axial stresses in the friction module of the shock absorber (Figure 1), then they reach their maximum absolute values in the planes of the ends of the filler (at the edges of the contact zone), decreasing with distance from these planes.

The displacement of the piston at this stage is a linear function of p and is calculated by the following formula:

$$\delta^I = u_\zeta^I(0) = \frac{pa}{E}\frac{2\varepsilon}{1+2\varepsilon}\frac{1-e^{-\lambda}}{\lambda}. \tag{19}$$

During the operation of the shock absorber, structural energy dissipation is present only in the areas of mutual sliding of the filler and the shell. Relation (19) describes the portion of the loading diagram (or structural hysteresis loop) corresponding to the initial loading. The linearity of this expression means that at this stage the loading of the shock absorber, the adhesion in the contact pair is not achieved.

3.2. The Stage of Shock Absorber Unloading. At this stage, the shock absorber load parameters change $p_{\max} \geq p \geq 0$, $\dot{p} < 0$. At the beginning of this stage, the unloading of the structure occurs in the mode of partial reverse sliding. The segment $\zeta \in [0,1]$ is divided into two areas: $\zeta \in [0,\alpha]$–the reverse sliding area, where $\partial u_\zeta/\partial p < 0$; $\zeta \in [\alpha,1]$–adhesion area, where $\partial u_\zeta/\partial p = 0$. The coordinate of the point of delimitation of the areas is unknown.

In the adhesion zone, there is an old pattern of stress and displacement distribution, which was achieved at the end of the previous stage:

$$\begin{aligned}
\sigma^{II}(\zeta) &= \sigma^I(\zeta)|_{p=p_{\max}},\\
\tau^{II}(\zeta) &= \tau^I(\zeta)\big|_{p=p_{\max}},\\
\sigma_\zeta^{II}(\zeta) &= \sigma^I(\zeta)\big|_{p=p_{\max}},\\
\zeta &\in [\alpha,1].
\end{aligned} \tag{20}$$

In the sliding zone, shear stresses change their direction to the opposite. Changing a parameter λ, we got:

$$\begin{aligned}
\sigma^{II}(\zeta) &= -\frac{p}{1+2\varepsilon}e^{\lambda\zeta},\\
\tau^{II}(\zeta) &= \frac{fp}{1+2\varepsilon}e^{\lambda\zeta},\\
\sigma_\zeta^{II}(\zeta) &= -pe^{\lambda\zeta},\\
\zeta &\in [0,\alpha].
\end{aligned} \tag{21}$$

Having ensured the fulfillment of condition (12), we found the coordinate of the point of delimitation of the areas of reverse sliding and adhesion

$$\alpha = \frac{1}{\lambda}\ln\left(\frac{p_{\max}}{p}\right)^{(1/2)}. \tag{22}$$

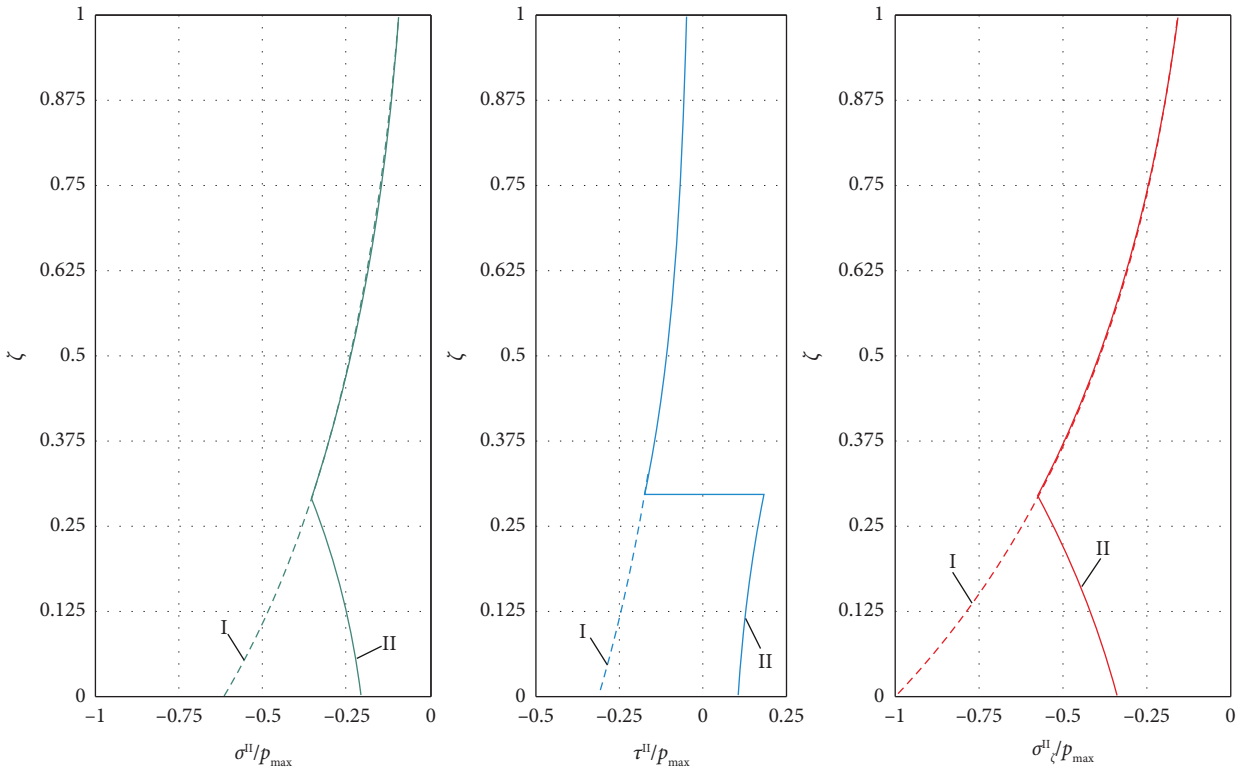

Figure 5: Stress distribution at the unloading stage (mode of partial sliding).

Stress graphs are shown in Figure 5 (hereinafter, the solid lines will represent the results of the current stage of loading or unloading, and the dashed lines will represent the results of the previous stages).

The described unloading process takes place until the point α reaches the upper limit $\zeta = 1$. From the condition $0 \le \alpha \le 1$, we find the corresponding range of pressure change: $e^{-2\lambda} p_{max} \le p \le p_{max}$, where $e^{-2\lambda}$ is a characteristic value of the cycle asymmetry coefficient p. Piston displacement in this loading range

$$\delta^{II} = \delta^{I}_{max} - \frac{a}{E}\frac{2\varepsilon}{1+2\varepsilon}\frac{1}{\lambda}\left(\sqrt{p_{max}} - \sqrt{p}\right)^2 \text{ at } e^{-2\lambda} p_{max} \le p \le p_{max}. \quad (23)$$

When the pressure under the piston drops to $p = e^{-2\lambda} p_{max}$, reverse sliding conditions will be satisfied on the entire contact surface $\zeta \in (0, 1]$. In this case, in the unloading range $0 \le p \le e^{-2\lambda} p_{max}$, formula (21) will be true. The characteristic stress distribution corresponding to this episode of unloading is shown in Figure 6. We will find the piston draft by the following formula:

$$\delta^{II} = \frac{pa}{E}\frac{2\varepsilon}{1+2\varepsilon}\frac{e^{\lambda}-1}{\lambda} \text{ at } 0 \le p \le e^{-2\lambda} p_{max}. \quad (24)$$

Consequently, the beginning of the unloading stage is characterized by the fact that nonunilateral sliding conditions are satisfied on the contact surfaces (Figure 5). In other words, the contact surface is divided into areas in which the velocity of the mutual displacement of the contacting bodies and, consequently, the contact stresses have opposite symbols. Formula (23) gives us a nonlinear relationship between piston displacement and loading. Toward the end of the unloading stage, one-sided sliding is achieved on the contact surfaces (Figure 6), and formula (24) indicates that the unloading section of the deformation diagram will always end in a straight line.

3.3. The Stage of Repeated Loading of the Shock Absorber. Shock absorber load parameters $p_{min} \le p \le p_{max}$, $\dot{p} > 0$. Depending on the value p_{min}, two cases are possible: $s \ge e^{-2\lambda}$ and $s \le e^{-2\lambda}$. Let's consider each of them in turn.

Let $1 \ge s \ge e^{-2\lambda}$. In this case, at the beginning of the repeated loading stage, we have direct sliding in the piston zone $\zeta \in [0, \beta]$ and the situation of the end of the preliminary stage in the region $\zeta \in [\beta, 1]$. The coordinate of the point of delimitation of the areas β is unknown.

In the adhesion zone $((\partial u_{\zeta}/\partial p = 0), \zeta \in [\beta, 1])$, stress is obtained from expressions (21) at $p = p_{min}$:

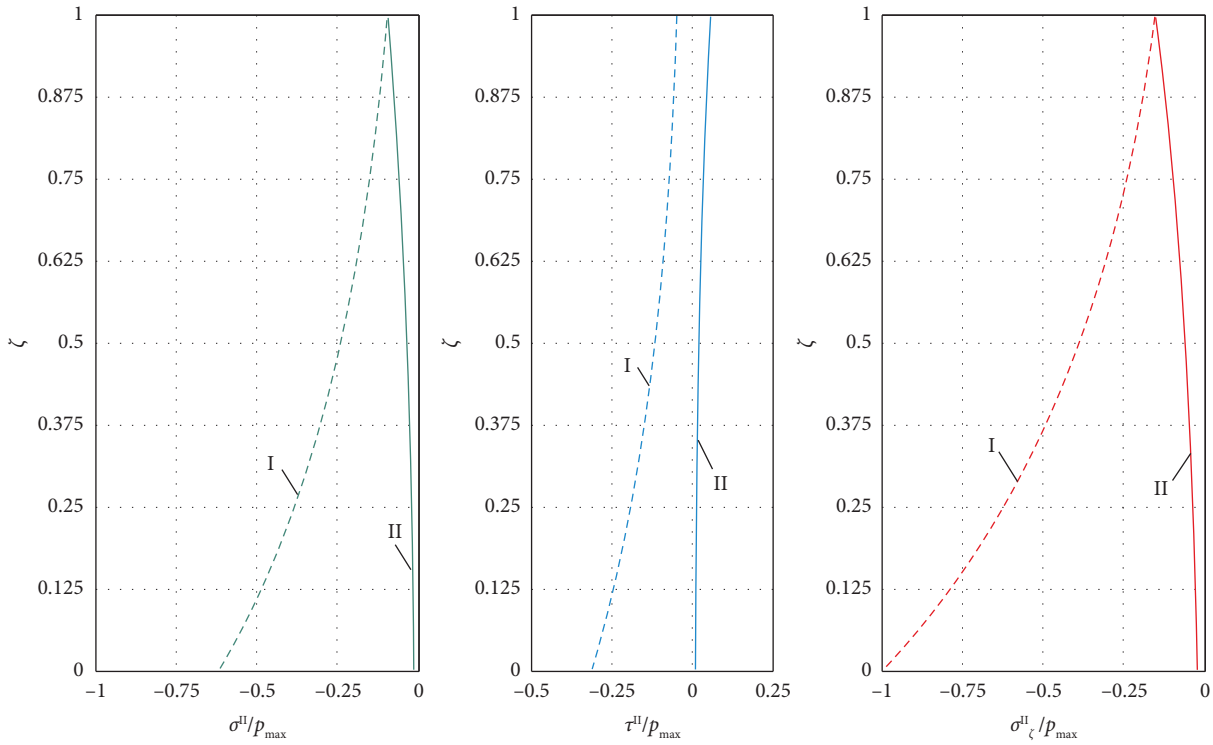

Figure 6: Stress distribution at the unloading stage (full sliding mode).

$$\sigma^{III}(\zeta) = \sigma^{II}(\zeta)\Big|_{p=p_{\min}} = \begin{cases} -\dfrac{p_{\min}}{1+2\varepsilon}e^{\lambda\zeta}, & \zeta \in [\beta, \alpha], \\ -\dfrac{p_{\max}}{1+2\varepsilon}e^{-\lambda\zeta}, & \zeta \in [\alpha, 1], \end{cases}$$

$$\tau^{III}(\zeta) = \tau^{II}(\zeta)\Big|_{p=p_{\min}} = \begin{cases} \dfrac{f p_{\min}}{1+2\varepsilon}e^{\lambda\zeta}, & \zeta \in [\beta, \alpha], \\ -\dfrac{f p_{\max}}{1+2\varepsilon}e^{-\lambda\zeta}, & \zeta \in [\alpha, 1], \end{cases}$$

$$\sigma^{III}_{\zeta}(\zeta) = \sigma^{II}_{\zeta}(\zeta)\Big|_{p=p_{\min}} = \begin{cases} -p_{\min}e^{\lambda\zeta}, & \zeta \in [\beta, \alpha], \\ -p_{\max}e^{-\lambda\zeta}, & \zeta \in [\alpha, 1]. \end{cases} \tag{25}$$

In the sliding zone $((\partial u_{\zeta}/\partial p = 0), \zeta \in [0, \beta])$, stress distributions are described by formula (18):

$$\begin{aligned} \sigma^{III}(\zeta) &= \sigma^{I}(\zeta), \\ \tau^{III}(\zeta) &= \tau^{I}(\zeta), \\ \sigma^{III}_{\zeta}(\zeta) &= \sigma^{I}_{\zeta}(\zeta), \\ \zeta &\in [0, \beta]. \end{aligned} \tag{26}$$

From the condition of continuity of axial stresses, we find the boundary of regions with opposite symbols of contact stresses

$$\beta = \frac{1}{\lambda}\ln\left(\frac{p}{p_{\min}}\right)^{1/2}. \tag{27}$$

Results (20) and (21) are graphically presented in Figure 7.

It is noteworthy that there are three regions at once on the contact surface. The difference between them lies in the fact that in each two adjacent areas, the tangential contact stresses have opposite symbols. It should be noted that the number of such areas for an arbitrary number of loading cycles with an arbitrary amplitude can be greater (this depends on the history of the loading).

The described process takes place until the point β reaches the point α (until the curves III are aligned with the curves I). This moment corresponds to the end of the cycle $(p = p_{\max})$.

Finally, the displacement of the piston at $1 \geq s \geq e^{-2\lambda}$ is determined by the following formula:

$$\delta^{III} = \delta^{II}_{\min} + \frac{a}{E}\frac{2\varepsilon}{1+2\varepsilon}\frac{1}{\lambda}\left(\sqrt{p} - \sqrt{p_{\min}}\right)^2. \tag{28}$$

Let now $0 \leq s \leq e^{-2\lambda}$. Then, in the zone of direct sliding $\zeta \in [0, \beta]$, dependencies (26) take place, and in the adhesion region $\zeta \in [\beta, 1]$, stress state (21) recorded at the end of unloading:

$$\begin{aligned} \sigma^{III}(\zeta) &= \sigma^{II}(\zeta)\Big|_{p=p_{\min}} = -\frac{p_{\min}}{1+2\varepsilon}e^{\lambda\zeta}, \\ \tau^{III}(\zeta) &= \tau^{II}(\zeta)\Big|_{p=p_{\min}} = \frac{f p_{\min}}{1+2\varepsilon}e^{\lambda\zeta}, \\ \sigma^{III}_{\zeta}(\zeta) &= \sigma^{II}_{\zeta}(\zeta)\Big|_{p=p_{\min}} = -p_{\min}e^{\lambda\zeta}, \zeta \in [\beta, 1]. \end{aligned} \tag{29}$$

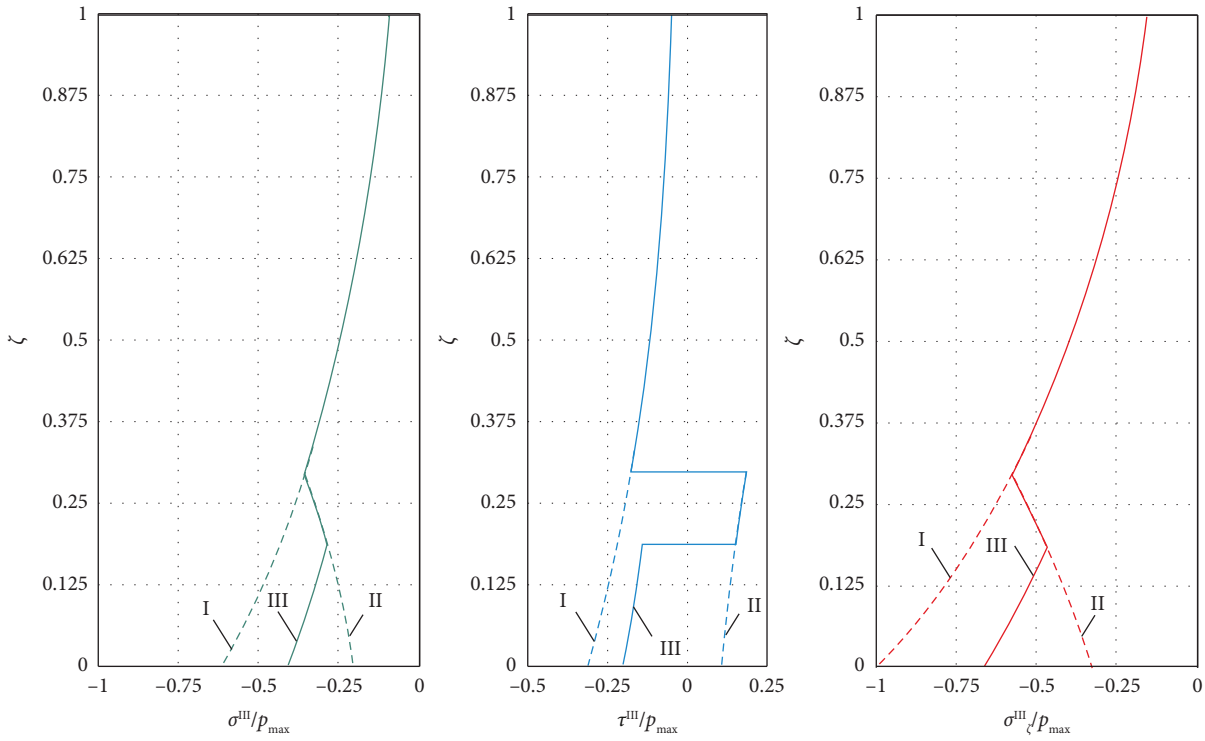

FIGURE 7: Stress distribution at the repeated loading stage at $1 \geq s \geq e^{-2\lambda}$.

To calculate the parameter β and piston draft at this stage, formulas (27) and (28) are preserved, respectively. Figure 8 illustrates the distribution of stresses characteristic of the situation under consideration.

This case is realized until the point β reaches the upper edge of the gap $[0, 1]$, which in terms of loading means $p_{min} \leq p \leq e^{2\lambda} p_{min}$. When $p = e^{2\lambda} p_{min}$ again, we enter the loading mode with full direct sliding on the entire contact surface.

3.4. Analytical Method of Drawing the Deformation Diagram of the Shell Shock Absorber. Let us summarize the study by bringing together expressions that describe all stages of the loading cycle. Let us denote $c_1 = (\pi R^2 E/a)(1 + 2\varepsilon/2\varepsilon)$ as linear rigidity of the conservative subsystem "shell-filler."

Then, based on formulas (14), (15), (17), (23), (24), and (28), we obtain the hysteresis loop equation in implicit form (dependences of δ on $Q_1 = Q - c_2\delta$).

For active loading,

$$\delta^I = \frac{Q - c_2\delta^I}{c_1} \frac{1 - e^{-\lambda}}{\lambda}, 0 \leq Q - c_2\delta^I \leq Q_{max} - c_2\delta^I_{max}. \quad (30)$$

For unloading,

$$\delta^{II} = \begin{cases} \delta^I_{max} - \frac{1}{c_1\lambda}\left(\sqrt{Q_{max} - c_2\delta^I_{max}} - \sqrt{Q - c_2\delta^{II}}\right)^2, \\ Q_{max} - c_2\delta^I_{max} \geq Q - c_2\delta^{II} \geq e^{-2\lambda}\left(Q_{max} - c_2\delta^I_{max}\right), \\ \frac{Q - c_2\delta^{II}}{c_1} \frac{e^{\lambda} - 1}{\lambda}, e^{-2\lambda}\left(Q_{max} - c_2\delta^I_{max}\right) \geq Q - c_2\delta^{II} \geq 0. \end{cases} \quad (31)$$

For repeated loading,

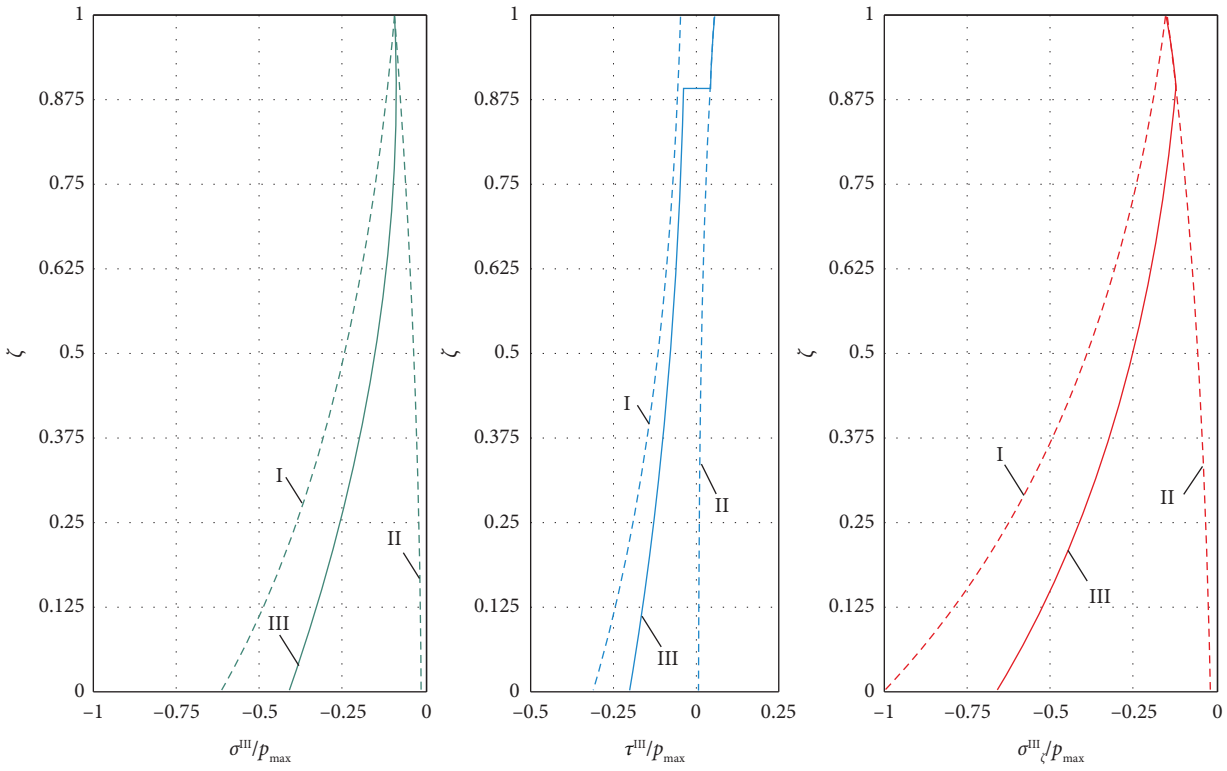

Figure 8: Stress distribution at the repeated loading stage at $0 \le s \le e^{-2\lambda}$.

$$\delta^{III} = \begin{cases} \delta^{II}_{\min} + \dfrac{1}{c_1\lambda}\left(\sqrt{Q - c_2\delta^{III}} - \sqrt{Q_{\min} - c_2\delta^{II}_{\min}}\right)^2, \\ Q_{\min} - c_2\delta^{II}_{\min} \le Q - c_2\delta^{III} \le \min\left\{\dfrac{\left(Q_{\min} - c_2\delta^{II}_{\min}\right)}{e^{-2\lambda}}, Q_{\max} - c_2\delta^{I}_{\max}\right\}, \\ \dfrac{Q - c_2\delta^{III}}{c_1}\dfrac{1 - e^{-\lambda}}{\lambda}, \\ \min\left\{\dfrac{\left(Q_{\min} - c_2\delta^{II}_{\min}\right)}{e^{-2\lambda}}, Q_{\max} - c_2\delta^{I}_{\max}\right\} \le Q - c_2\delta^{III} \le Q_{\max} - c_2\delta^{I}_{\max}. \end{cases} \tag{32}$$

Solving equations (30)–(32) with respect to Q, we found explicit expressions of Q by means of δ at all stages of the cycle:

For active loading,

$$Q^{I} = \left(c_1\frac{\lambda}{1 - e^{-\lambda}} + c_2\right)\delta, 0 \le \delta \le \delta_{\max}. \tag{33}$$

For unloading,

$$Q^{II} = \begin{cases} \left(\sqrt{Q^{I}_{\max} - c_2\delta_{\max}} - \sqrt{c_1\lambda\left(\delta_{\max} - \delta\right)}\right)^2 + c_2\delta, \delta_{\max} \ge \delta \ge e^{-\lambda}\delta_{\max}, \\ \left(c_1\dfrac{\lambda}{e^{\lambda} - 1} + c_2\right)\delta, e^{-\lambda}\delta_{\max} \ge \delta \ge 0. \end{cases} \tag{34}$$

For repeated loading,

$$Q^{III} = \begin{cases} \left(\sqrt{Q^{II}_{\min} - c_2\delta_{\min}} + \sqrt{c_1\lambda\left(\delta - \delta_{\min}\right)}\right)^2 + c_2\delta, \delta_{\min} \le \delta \le \min\left\{e^{\lambda}\delta_{\min}, \delta_{\max}\right\}, \\ \left(c_1\dfrac{\lambda}{1-e^{-\lambda}} + c_2\right)\delta, \ \min\left\{e^{\lambda}\delta_{\min}, \delta_{\max}\right\} \le \delta \le \delta_{\max}. \end{cases} \tag{35}$$

In contrast to previous works [41, 42, 83], in which the phenomenon of structural hysteresis in shell dampers is described in terms of the power cycle $(Q_{\min}, Q_{\max})$, the equations (33)–(35) obtained here present the nonconservative properties of the damper in terms of the kinematic cycle $(\delta_{\min}, \delta_{\max})$. This approach actually made it possible to study energy dissipation in the parallel connection of the nonlinear and the linear element.

According to expressions (33)–(35), a structural damping loop was built (Figure 9). Still here, $\lambda \approx 1.86$, in addition, value $c_1/c_2 = 5$ was recorded.

Let us move on to the assessment of permissible loadings. Let $Q = Q_{\max}$. The analysis showed that the most dangerous place in the open shell is a point with coordinates $(R, \pi, 0)$. Indeed, here the maximum hoop stress from bending and the greatest modulus axial stress from compression are achieved:

$$\begin{aligned} \sigma^{\text{shell}}_{\vartheta\max} &= \max_{\vartheta\in[0,2\pi]} \frac{1}{h}\left(N_{\vartheta} - \frac{6}{h}M_{\vartheta}\right) = 2\frac{p_{\max}}{1+2\varepsilon}\frac{R}{h}\left(1+6\frac{R}{h}\right) \approx \frac{Q_{1\max}}{\pi R^2}\frac{12}{1+2\varepsilon}\left(\frac{R}{h}\right)^2, \\ \sigma^{\text{shell}}_{\zeta\min} &= -\frac{Q_{2\max}}{2\pi R h}. \end{aligned} \tag{36}$$

The strength of the bearing links of the structure will be ensured if the irregularities are true:

$$\begin{aligned} \max \sigma^{\text{shell}}_{eq} &\equiv \sigma^{\text{shell}}_{\vartheta\max} - \sigma^{\text{shell}}_{\zeta\min} \le [\sigma]^{\text{shell}}, \\ \max\left|Q_2^{\text{spring}}\right| &\equiv Q_{2\max} \le [Q]^{\text{spring}}. \end{aligned} \tag{37}$$

Here, $\sigma^{\text{shell}}_{eq}$ is Tresca equivalent stress, $[\sigma]^{\text{shell}}$ is an allowable stress for the shell material, and $[Q]^{\text{spring}}$ is an allowable compression force for the spring.

From formulas (13), (14), and (33), it follows that the maximum loadings on the filler and on the spring are divided in proportion to the corresponding rigidities of the subsystems:

$$\begin{aligned} Q_{1\max} &= \frac{c_1\left(\lambda/\left(1-e^{-\lambda}\right)\right)}{c_1\left(\lambda/\left(1-e^{-\lambda}\right)\right)+c_2}Q_{\max}, \\ Q_{2\max} &= \frac{c_2}{c_1\left(\lambda/\left(1-e^{-\lambda}\right)\right)+c_2}Q_{\max}. \end{aligned} \tag{38}$$

Then, from relation (36)–(38), we obtain the conditions for the safe operation of the shock absorber in the form of restrictions on the external loading:

$$\begin{aligned} Q_{\max} &\le [\sigma]^{\text{shell}}\pi R^2\left(\frac{c_1\left(\lambda/\left(1-e^{-\lambda}\right)\right)}{c_1\left(\lambda/\left(1-e^{-\lambda}\right)\right)+c_2}\frac{12}{1+2\varepsilon}\left(\frac{R}{h}\right)^2 + \frac{c_2}{c_1\left(\lambda/\left(1-e^{-\lambda}\right)\right)+c_2}\frac{R}{2h}\right)^{-1}, \\ Q_{\max} &\le [Q]^{\text{spring}}\frac{c_1\left(\lambda/\left(1-e^{-\lambda}\right)\right)+c_2}{c_2}. \end{aligned} \tag{39}$$

Which of the inequalities (39) is stronger depends on the values of the geometric and mechanical parameters of all structural elements of the shock absorber.

Therefore, formulas (33)–(35) and (39) are the main ones for the engineering calculation of a shock absorber and make it possible to construct a deformation diagram and

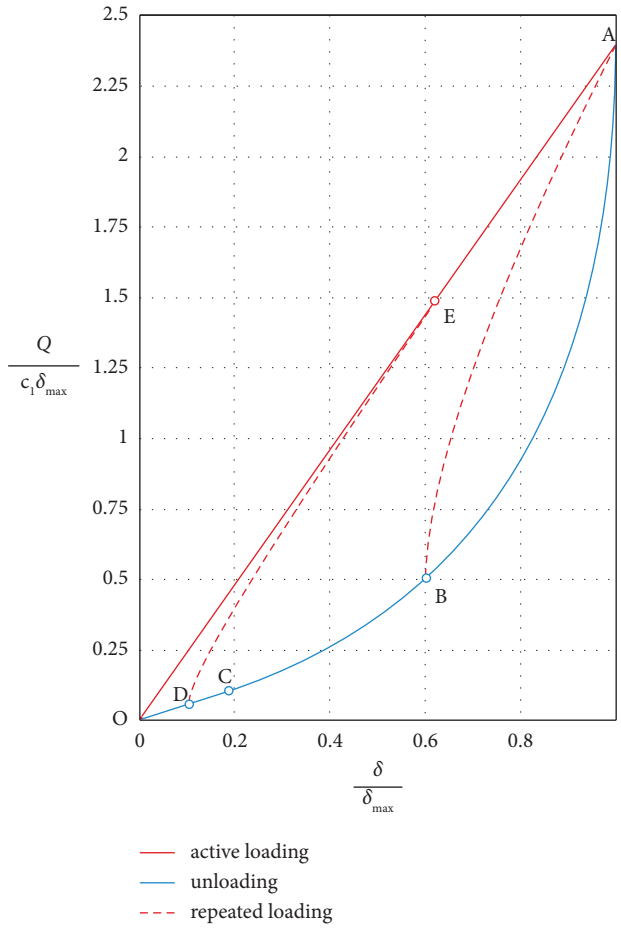

FIGURE 9: Diagram of the cyclic loading of the shock absorber: OA: active (initial) loading; ACO: unloading (here, AC is a nonlinear section, and CO is a linear section); BA or DEA: repeated loading.

determine the holding capacity of the device for any coefficient of loading cycle asymmetry.

4. Conclusions

The idea of using the bending strain of load-bearingthin-walled links for shell dampers and shock absorbers is quite fruitful and will form the basis of a number of technical solutions. It should be noted that the shell shock absorber has both damping and shock-absorbing properties. However, for the qualitative implementation of the theoretical concepts on which the principle of the operation of the shock absorber is based, its constituent elements must have certain characteristic properties. Open shell requires a combination of low rigidity with a sufficient level of strength and durability. For the directional transformation of displacements, the filler must easily change its shape. On the other hand, in order to cause the open shell to deform under contact pressure, the filler material must have a high bulk modulus. These requirements are met by elastomers, which are also capable of frequency-dependent energy dissipation. The tribological characteristics of the filler-shell contact pair are selected in order to ensure the level of structural damping required in a particular operational situation.

This study has three main innovation outcomes.

(1) A new design of the dry friction shock absorber is introduced. The device contains two spring sections and a friction module (an open shell with an elastic filler). The spring sections and the friction module work in parallel. The proposed shock absorber with compact transverse dimensions demonstrates good performance.

(2) To describe the deformation of a friction shock absorber, a mechanical-mathematical model of a shell with a cut along the generatrix, which is the main bearing link of the device under consideration, has been developed. An open isotropic shell was modeled by an equivalent continuous strongly orthotropic momentless shell. The elasticity characteristics of such an equivalent shell were determined on the basis of solving an additional problem of loading a cut shell with internal pressure.

(3) A technique for the quasistatic analysis of structural damping in nonmobile nonconservative shell systems with an elastic filler has been developed. The hysteresis loop for an open cylindrical shell with a deforming filler is described analytically. The

distribution of stresses at each stage of the cyclic loading was studied, and the permissible loading was determined at which the operation of the shock absorber would be safe.

Thus, the purpose of the study has been achieved. The results obtained make it possible to evaluate the behavior of friction shock absorbers with a working link in the form of an open cylindrical shell with an elastic filler and a spring connected in parallel under cyclic loading conditions and to carry out an engineering calculation of their rigidity and holding capacity, focused on the practical needs of use and efficient operation.

In future studies, it is advisable to study the effect of frictional heat generation and wear in the contact interface on the properties of the shock absorber during long-term operation.

The authors see good prospects for using the presented friction shock absorber in the mining, oil and gas, and construction industries.

Nomenclature

h: Shell thickness
R: Shell radius
r, ϑ, z: Coordinates of the cylindrical coordinate system
E_0: Modulus of elasticity of the open shell material
E_e: Modulus of elasticity of the equivalent shell
q: Internal pressure in the shell
N_ϑ: Tangential force
M_ϑ: Bending moment
Q_ϑ: Transverse force
$w(\vartheta)$: Function of shell deflections
$w^{(1)}$: Average deflection of the open shell
$w^{(2)}$: Average deflection of the equivalent shell
Q: External cyclic loading
Q_1: Filler loading
Q_2: Spring loading
p: Pressure under the piston
a: Filler length
ζ: Dimensionless coordinate
σ_ζ: Axial stresses in the filler
u: Axial displacement of the filler
σ: Normal contact stress
τ: Tangential contact stress
w: Radial displacement on the surface $r = R$ in the filler
E: Modulus of elasticity of the filler material
w_0: Radial displacement of the shell
u_0: Axial displacement of the shell
f: Coefficient of friction of the contact pair shell-filler
α, β: Coordinates of the points of delimitation of the areas of adhesion and sliding of the filler and shell
s: Cycle asymmetry coefficient
δ: Displacement of the shock absorber piston
λ: Parameter of exponential decay of axial and contact stresses
ε: Auxiliary dimensionless rigidity parameter
c_1: Linear rigidity of the conservative "shell-filler" subsystem
c_2: Coefficient of linear rigidity of the spring
u_2: Axial displacement of the spring
σ_ϑ: Hoop stress in the shell
$[Q]^{\text{spring}}$: Allowable compression force for the spring
$\sigma_{\text{eq}}^{\text{shell}}$: Tresca equivalent stress
$[\sigma]^{\text{shell}}$: Allowable stress for the shell material.

Data Availability

All results are included in the article, and there are no additional hyperlinks.

Conflicts of Interest

The authors declare that they have no conflicts of interest.

References

[1] Z.-D. Xu, Z.-H. Chen, X.-H. Huang et al., "Recent advances in multi-dimensional vibration mitigation materials and devices," *Frontiers in Materials*, vol. 6, p. 143, 2019.

[2] M. Rigacci, R. Sato, and K. Shirase, "Evaluating the influence of mechanical system vibration characteristics on servo motor efficiency," *Precision Engineering*, vol. 72, pp. 680–689, 2021.

[3] M. Dutkiewicz, "Models of strong wind acting on buildings and infrastructure," *IOP Conference Series: Materials Science and Engineering*, vol. 471, no. 5, Article ID 052030, 2019.

[4] O. Bazaluk, O. Slabyi, V. Vekeryk, A. Velychkovych, L. Ropyak, and V. Lozynskyi, "A technology of hydrocarbon fluid production intensification by productive stratum drainage zone reaming," *Energies*, vol. 14, no. 12, p. 3514, 2021.

[5] L. Ya. Ropyak, T. O. Pryhorovska, and K. H. Levchuk, "Analysis of materials and modern technologies for PDC drill bit manufacturing," *Uspehi Fiziki Metallov*, vol. 20, no. 2, pp. 274–301, 2020.

[6] D. Bukreieva, P. Saik, V. Lozynskyi, E. Cabana, and O. Stoliarska, "Assessing the effectiveness of innovative projects implementation in the development of coal deposits by geotechnology of underground gasification," *IOP Conference Series: Earth and Environmental Science*, vol. 970, no. 1, Article ID 012031, 2022.

[7] A. S. Velichkovich and T. M. Dalyak, "Assessment of stressed state and performance characteristics of jacketed spring with a cut for drill shock absorber," *Chemical and Petroleum Engineering*, vol. 51, no. 3-4, pp. 188–193, 2015.

[8] A. Velychkovych, I. Petryk, and L. Ropyak, "Analytical study of operational properties of a plate shock absorber of a sucker-rod string," *Shock and Vibration*, vol. 2020, Article ID 3292713, 7 pages, 2020.

[9] R. S. Silva, T. G. Ritto, and M. A. Savi, "Shape memory alloy couplers applied for torsional vibration attenuation of drill-string systems," *Journal of Petroleum Science and Engineering*, vol. 202, p. 202, Article ID 108546, 2021.

[10] H. Gong, J. Liu, and X. Ding, "Study on local slippage accumulation between thread contact surfaces and novel anti-

loosening thread designs under transversal vibration," *Tribology International*, vol. 153, Article ID 106558, 2021.

[11] V. Kopei, O. Onysko, V. Panchuk, L. Pituley, and I. Schuliar, "Influence of working height of a thread profile on quality indicators of the drill-stringtool-joint. Advanced manufacturing processes III. InterPartner 2021," *Lecture Notes in Mechanical Engineering 2022*, Springer, Cham, 2021.

[12] L. Ya. Ropyak, V. S. Vytvytskyi, A. S. Velychkovych, T. O. Pryhorovska, and M. V. Shovkoplias, "Study on grinding mode effect on external conical thread quality," *IOP Conference Series: Materials Science and Engineering*, vol. 1018, no. 1, Article ID 012014, 2021.

[13] W. Sarwar and R. Sarwar, "Vibration control devices for building structures and installation approach: a review," *Civil and Environmental Engineering Reports*, vol. 29, no. 2, pp. 74–100, 2019.

[14] I. P. Shats'kyi, V. M. Shopa, and A. S. Velychkovych, "Development of full-strength elastic element section with open shell," *Strength of Materials*, vol. 53, no. 2, pp. 277–282, 2021.

[15] M. Dutkiewicz, I. Golebiowska, I. Shatskyi, V. Shopa, and A. Velychkovych, "Some aspects of design and application of inertial dampers," *MATEC Web of Conferences*, vol. 178, Article ID 06010, 2018.

[16] X. Yuan, T. Tian, H. Ling, T. Qiu, and H. He, "review on structural development of magnetorheological fluid damper," *A Shock and Vibration*, vol. 2019, Article ID 1498962, 10 pages, 2019.

[17] Z. Wang, T. Zhang, Z. Zhang, Y. Yuan, and Y. Liu, "A high-efficiency regenerative shock absorber considering twin ball screws transmissions for application in range-extended electric vehicles," *Energy and Built Environment*, vol. 1, no. 1, pp. 36–49, 2020.

[18] B. Yan, X. Wang, Z. Wang, C. Wu, and W. Zhang, "Enhanced lever-type vibration isolator via electromagnetic shunt damping," *International Journal of Mechanical Sciences*, vol. 218, Article ID 107070, 2022.

[19] M. Miraglia, M. Tannous, F. Inglese, B. Brämer, M. Milazzo, and C. Stefanini, "Energy recovery from shock absorbers through a novel compact electro-hydraulic system architecture," *Mechatronics*, vol. 81, Article ID 102701, 2022.

[20] D. Guan, X. Cong, J. Li, P. Wang, Z. Yang, and X. Jing, "Theoretical modeling and optimal matching on the damping property of mechatronic shock absorber with low speed and heavy load capacity," *Journal of Sound and Vibration*, vol. 535, Article ID 117113, 2022.

[21] W. Salman, X. Zhang, H. Li et al., "A novel energy regenerative shock absorber for in-wheel motors in electric vehicles," *Mechanical Systems and Signal Processing*, vol. 181, Article ID 109488, 2022.

[22] N. Deshmukh, S. Ren, J. Mi, and L. Zuo, "Modeling and simulation of energy harvesting hydraulically interconnected shock absorber," *IFAC-PapersOnLine*, vol. 55, no. 37, pp. 229–234, 2022.

[23] S. Zhang, W. Shi, and Z. Chen, "Modeling and parameter identification of MR damper considering excitation characteristics and current," *Shock and Vibration*, vol. 202117 pages, Article ID 6691650, 2021.

[24] M. U. Shah and M. Usman, "An experimental study of tuned liquid column damper controlled multi-degree of freedom structure subject to harmonic and seismic excitations," *PLoS One*, vol. 17, no. 6, Article ID e0269910, 2022.

[25] M. U. Shah, M. Usman, S. H. Farooq, and M. Rizwan, "Spring-controlled modified tuned liquid column ball damper for vibration mitigation of structures," *Journal of Sound and Vibration*, vol. 545, Article ID 117443, 2023.

[26] M. U. Shah, M. Usman, In-Ho Kim, and S. Dawood, "Analytical and experimental investigations on the performance of tuned liquid column ball damper considering a hollow ball," *Structural Engineering & Mechanics*, vol. 83, pp. 655–669, 2022.

[27] Z. Lu, X. Chen, D. Zhang, and K. Dai, "Experimental and analytical study on the performance of particle tuned mass dampers under seismic excitation," *Earthquake Engineering & Structural Dynamics*, vol. 46, no. 5, pp. 697–714, 2017.

[28] X. Wu, X. Liu, J. Chen, K. Liu, and C. Pang, "Parameter optimization and application for the inerter-based tuned type dynamic vibration absorbers," *Buildings*, vol. 12, no. 6, p. 703, 2022.

[29] A. S. Velichkovich and S. V. Velichkovich, "Vibration-impact damper for controlling the dynamic drillstring conditions," *Chemical and Petroleum Engineering*, vol. 37, no. 3/4, pp. 213–215, 2001.

[30] Z. Lu, D. Wang, and Y. Zhou, "Experimental parametric study on wind-induced vibration control of particle tuned mass damper on a benchmark high-rise building," *The Structural Design of Tall and Special Buildings*, vol. 26, no. 8, p. e1359, 2017.

[31] S. Jaisee, F. Yue, and Y. H. Ooi, "A state-of-the-art review on passive friction dampers and their applications," *Engineering Structures*, vol. 235, Article ID 112022, 2021.

[32] I. Shatskyi and A. Velychkovych, "Increase of compliance of shock absorbers with cut shells," *IOP Conference Series: Materials Science and Engineering*, vol. 564, no. 1, Article ID 012072, 2019.

[33] L. Gagnon, M. Morandini, and G. L. Ghiringhelli, "A review of friction damping modeling and testing," *Archive of Applied Mechanics*, vol. 90, no. 1, pp. 107–126, 2020.

[34] M. B. dos Santos, H. T. Coelho, F. P. Lepore Neto, and J. Mahfoud, "Assessment of semi-active friction dampers," *Mechanical Systems and Signal Processing*, vol. 94, pp. 33–56, 2017.

[35] N. Maureira-Carsalade, M. Villagrán-Valenzuela, D. Sanzana-Jara, and A. Roco-Videla, "Proof of concept of a novel frictional shock absorber; analytical model and experimental analysis," *Engineering Structures*, vol. 230, Article ID 111657, 2021.

[36] Z. Huang, J. Tan, C. Liu, and X. Lu, "Dynamic characteristics of a segmented supercritical driveline with flexible couplings and dry friction dampers," *Symmetry*, vol. 13, no. 2, p. 281, 2021.

[37] H. S. Wahad, A. Tudor, M. Vlase, N. Cerbu, and K. A. Subhi, "The effect of friction in coulombian damper," *IOP Conference Series: Materials Science and Engineering*, vol. 174, Article ID 012021, 2017.

[38] M. Paronesso and D. G. Lignos, "Experimental study of sliding friction damper with composite materials for earthquake resistant structures," *Engineering Structures*, vol. 248, Article ID 113063, 2021.

[39] A. A. Bedzir, I. P. Shatskii, and V. M. Shopa, "Nonideal contact in a composite shell structure with a deformable filler," *International Applied Mechanics*, vol. 31, no. 5, pp. 351–354, 1995.

[40] V. M. Shopa, I. P. Shatskii, and I. I. Popadyuk, "Elementary calculation of structural damping in shell springs," *Soviet Engineering Research*, vol. 9, no. 3, pp. 42–44, 1989.

[41] I. Y. Popadyuk, I. P. Shats'kyi, V. M. Shopa, and A. S. Velychkovych, "Frictional interaction of a cylindrical

shell with deformable filler under nonmonotonic loading," *Journal of Mathematical Sciences*, vol. 215, no. 2, pp. 243–253, 2016.

[42] I. Yo. Popadyuk, I. P. Shatskyi, and V. M. Shopa, *Mechanics of Frictional Contact of Shells with Deformable Filler*Ivano-Frankivs'k, Fakel, 2003.

[43] I. Shatskyi, L. Ropyak, and A. Velychkovych, "Model of contact interaction in threaded joint equipped with spring-loaded collet," *Engineering Solid Mechanics*, vol. 8, no. 4, pp. 301–312, 2020.

[44] L. Ya. Ropyak, M. V. Makoviichuk, I. P. Shatskyi, I. M. Pritula, L. O. Gryn, and V. O. Belyakovskyi, "Stressed state of laminated interference-absorption filter under local loading," *Functional Materials*, vol. 27, no. 3, pp. 638–642, 2020.

[45] A. Velychkovych, L. Ropyak, and O. Dubei, "Strength analysis of a two-layerPETF-concrete column with allowance for contact interaction between layers," *Advances in Materials Science and Engineering*, vol. 2021, Article ID 4517657, 10 pages, 2021.

[46] O. Bazaluk, A. Velychkovych, L. Ropyak, M. Pashechko, T. Pryhorovska, and V. Lozynskyi, "Influence of heavy weight drill pipe material and drill bit manufacturing errors on stress state of steel blades," *Energies*, vol. 14, p. 4198, 2021.

[47] B. Pelekhan, M. Dutkiewicz, I. Shatskyi, A. Velychkovych, M. Rozhko, and L. Pelekhan, "Analytical modeling of the interaction of a four implant-supported overdenture with bone tissue," *Materials*, vol. 15, no. 7, p. 2398, 2022.

[48] A. Chuzhak, V. Sulyma, L. Ropyak, A. Velychkovych, and V. Vytvytskyi, "Mathematical modelling of destabilization stress factors of stable-elastic fixation of distal trans- and suprasyndesmotic fibular fractures," *Journal of Healthcare Engineering*, vol. 2021, Article ID 6607364, 8 pages, 2021.

[49] V. L. Popov, *Contact Mechanics and Friction: Physical Principles and Applications*, Springer-Verlag, Berlin, Heidelberg, 1st edition, 2010.

[50] E. Balalayeva, V. Kukhar, V. Artiukh, V. V. Filatov, and O. Simonova, "Computer aided simulation of behavior of extrusion press ram jointly with rotary elastic compensator," *Advances in Intelligent Systems and Computing*, vol. 983, pp. 475–488, 2019.

[51] A. S. Velychkovych, A. V. Andrusyak, T. O. Pryhorovska, and L. Y. Ropyak, "Analytical model of oil pipeline overground transitions, laid in mountain areas," *Oil & Gas Science and Technology – Revue d'IFP Energies nouvelles*, vol. 74, p. 65, 2019.

[52] I. Shatskyi, I. Vytvytskyi, M. Senyushkovych, and A. Velychkovych, "Modelling and improvement of the design of hinged centralizer for casing," *IOP Conference Series: Materials Science and Engineering*, vol. 564, no. 1, Article ID 012073, 2019.

[53] M. Dutkiewicz, T. Dalyak, I. Shatskyi, T. Venhrynyuk, and A. Velychkovych, "Stress analysis in damaged pipeline with composite coating," *Applied Sciences*, vol. 11, no. 22, Article ID 10676, 2021.

[54] R. Liu, T. Zhang, X. J. Wu, and C. H. Wang, "Crack closure effect on stress intensity factors of an axially and a circumferentially cracked cylindrical shell," *International Journal of Fracture*, vol. 125, no. 3/4, pp. 227–248, 2004.

[55] I. P. Shats'kyi, "Closure of a longitudinal crack in a shallow cylindrical shell in bending," *Materials Science*, vol. 41, no. 2, pp. 186–191, 2005.

[56] I. P. Shats'kyi and M. V. Makoviichuk, "Analysis of the limiting state of cylindrical shells with cracks with regard for the contact of crack lips," *Strength of Materials*, vol. 41, no. 5, pp. 560–564, 2009.

[57] I. P. Shatskii and N. V. Makoviichuk, "Effect of closure of collinear cracks on the stress-strain state and the limiting equilibrium of bent shallow shells," *Journal of Applied Mechanics and Technical Physics*, vol. 52, no. 3, pp. 464–470, 2011.

[58] K. M. Dovbnya and N. A. Shevtsova, "Studies on the stress state of an orthotropic shell of arbitrary curvature with the through crack under bending loading," *Strength of Materials*, vol. 46, no. 3, pp. 345–349, 2014.

[59] I. P. Shatskii, "Contact of the edges of the slit in the plate in combined tension and bending," *Soviet Materials Science*, vol. 25, no. 2, pp. 160–165, 1989.

[60] I. P. Shats'kyi and V. V. Perepichka, "Limiting state of a semi-infinite plate with edge crack in bending with tension," *Materials Science*, vol. 40, no. 2, pp. 240–246, 2004.

[61] I. P. Shats'kyi and M. V. Makoviichuk, "Contact interaction of crack lips in shallow shells in bending with tension," *Materials Science*, vol. 41, no. 4, pp. 486–494, 2005.

[62] A. Nobili, E. Radi, and L. Lanzoni, "A cracked infinite Kirchhoff plate supported by a two-parameter elastic foundation," *Journal of the European Ceramic Society*, vol. 34, no. 11, pp. 2737–2744, 2014.

[63] I. P. Shats'kyi and M. V. Makoviichuk, "Contact interaction of the crack edges in the case of bending of a plate with elastic support," *Materials Science*, vol. 39, no. 3, pp. 371–376, 2003.

[64] F. Marques, P. Flores, J. C. P. Claro, and H. M. Lankarani, "Modeling and analysis of friction including rolling effects in multibody dynamics: a review," *Multibody System Dynamics*, vol. 45, no. 2, pp. 223–244, 2019.

[65] V. Moisyshyn and K. Levchuk, "Investigation on releasing of a stuck drill string by means of a mechanical jar," *Oil & Gas Science and Technology – Revue d'IFP Energies nouvelles*, vol. 72, no. 5, pp. 27–35, 2017.

[66] I. P. Shatskii and V. V. Perepichka, "Shock-wave propagation in an elastic rod with a viscoplastic external resistance," *Journal of Applied Mechanics and Technical Physics*, vol. 54, no. 6, pp. 1016–1020, 2013.

[67] I. Shatskyi and V. Perepichka, "Problem of dynamics of an elastic rod with decreasing function of elastic-plastic external resistance," in *Dynamical Systems in Applications, Proceedings of the DSTA 2017, Lodz, Poland, 11–14 December 2017*, J. Awrejcewicz, Ed., Springer, Cham, Switzerland, 2018.

[68] S. Isić, S. Mehremić, I. Karabegović, and E. Husak, "Systems for passive and active vibration damping new technologies, development and application II. NT," *Lecture Notes in Networks and Systems*, Springer, Cham, 2019.

[69] M. Dutkiewicz and M. Machado, "Spectral element method in the analysis of vibrations of overhead transmission line in damping environment," *Structural Engineering & Mechanics*, vol. 71, pp. 291–303, 2019.

[70] S. V. Velichkovich, I. I. Popadyuk, I. P. Shatskii, and V. M. Shopa, "Structural hysteresis in a shell-type vibration damper with distributed friction," *Strength of Materials*, vol. 23, no. 3, pp. 279–281, 1991.

[71] A. K. Mohamed, M. Yu. Zadorozhnyy, Y. Mansouri, and I. S. Golovin, "Magnetostriction and damping of forced vibrations in Fe-Cr-Mo-Al alloy," *Materials Letters*, vol. 314, Article ID 131863, 2022.

[72] M. Pańtak, B. Jarek, and K. Marecik, "Vibration damping in steel footbridges," *IOP Conference Series: Materials Science and Engineering*, vol. 419, Article ID 012029, 2018.

[73] M. A. Shaid Sujon, A. Islam, and V. K. Nadimpalli, "Damping and sound absorption properties of polymer matrix composites: a review," *Polymer Testing*, vol. 104, Article ID 107388, 2021.

[74] K. T. Werkle, C. Menze, T. Stehle, and H.-C. Mohring, "Additively manufactured, particle-filled damping structures with magnetorheological fluids," *Procedia CIRP*, vol. 104, pp. 1418–1423, 2021.

[75] D. Li, H. Fang, and L. Duan, "High structural damping based on the internal snap-buckling mechanism of a continuous metal module," *Mechanics Research Communications*, vol. 105, Article ID 103514, 2020.

[76] M. Eugeni, F. Saltari, and F. Mastroddi, "Structural damping models for passive aeroelastic control," *Aerospace Science and Technology*, vol. 118, Article ID 107011, 2021.

[77] J. S. Love and T. C. Haskett, "Measuring inherent structural damping of structure-TMD systems," *Engineering Structures*, vol. 196, Article ID 109300, 2019.

[78] A. Velichkovich, T. Dalyak, and I. Petryk, "Slotted shell resilient elements for drilling shock absorbers," *Oil & Gas Science and Technology – Revue d'IFP Energies nouvelles*, vol. 73, p. 34, 2018.

[79] A. Velychkovych, O. Bedzir, and V. Shopa, "Laboratory experimental study of contact interaction between cut shells and resilient bodies," *Engineering Solid Mechanics*, vol. 9, no. 4, pp. 425–438, 2021.

[80] A. Velychkovych, "Numerical model of interation of package of open shells with a weakly compressible filler in a friction shock absorber," *Engineering Solid Mechanics*, vol. 10, no. 3, pp. 287–298, 2022.

[81] I. Shatskyi, I. Popadyuk, and A. Velychkovych, "Hysteretic properties of shell dampers," in *Dynamical Systems in Applications, Proceedings of the DSTA 2017, Lodz, Poland, 11–14 December 2017*, J. Awrejcewicz, Ed., Springer, Cham, Switzerland, pp. 343–350, 2018.

[82] A. S. Velichkovich, I. I. Popadyuk, and V. M. Shopa, "Experimental study of shell flexible component for drilling vibration damping devices," *Chemical and Petroleum Engineering*, vol. 46, no. 9-10, pp. 518–524, 2011.

[83] M. Dutkiewicz, A. Velychkovych, I. Shatskyi, and V. Shopa, "Efficient model of the interaction of elastomeric filler with an open shell and a chrome-plated shaft in a dry friction damper," *Materials*, vol. 15, no. 13, p. 4671, 2022.